Effects of vaccination strategies in the SIR model with a quarantine extension

Author:

Yu-Pei Sung

Supervisor:

Jeroen Eijkens

June 29, 2023

Statement of Originality

This document is written by Student Yu-Pei Sung who declares to take full responsibility for the contents of this document. I declare that the text and the work presented in this document are original and that no sources other than those mentioned in the text and its references have been used in creating it. UvA Economics and Business is responsible solely for the supervision of completion of the work and submission, not for the contents.

EFFECTS OF VACCINATION STRATEGIES IN THE SIR MODEL WITH A QUARANTINE EXTENSION

YU-PEI SUNG
Faculty of Economics and Business, University of Amsterdam

SUPERVISOR: JEROEN EIJKENS
Faculty of Economics and Business, University of Amsterdam

In this thesis, an extension of the SIR model which includes the quarantined states is concerned; it is able to address issues such as infected but undiagnosed cases and individuals uncooperative with the quarantine policy. Several vaccination strategies are applied in simulated networks in which the disease propagation is characterized by the extended SIR model. Among the strategies investigated, targeted vaccination is the most effective as to control the spread of the disease.

1. INTRODUCTION

Vaccination is a common control measure to battle infectious diseases (Yang and Atkinson (2008)). However, if there is a limited supply or a shortage of vaccines in a population, the question of how to reach maximum protection for the population given the constraint arises. For policy makers to determine the optimal allocation of vaccination resources, the dynamics of a disease, as well as the structure of social contacts in a given population should be taken into consideration, because immunization of susceptible individuals implies breaks of transmission routes between the susceptible and infective population (May and Anderson (1984)).

A popular approach to formulize the dynamics of an infectious disease is the susceptible-infected-recovered (SIR) model. The model could be extended in a way such that it could possibly characterize the changes in contact networks due to intervention of disease propagation. Firstly, the impact of undiagnosed cases could be incorporated in the model. In the case of COVID-19, the presence of asymptomatic cases of infection and the limited capacity of testing at the start of the pandemic led to a large number undetected cases (Brugnano et al. (2021)). The quarantine policies imposed by governments are therefore not functional on the undetected part of the infective population. Secondly, because of the nature of the virus, there exists a time

Supervisor: Jeroen Eijkens: j.eijkens@uva.nl

lag between one getting contaminated and them getting diagnosed of the disease (Brugnano et al. (2021)). By including these features when formulating the model, it is possible that the effectiveness of vaccination strategies could be evaluated more realistically.

The aim of this thesis is to compare the effectiveness of different vaccination strategies for an infectious disease that is spreading in a small-world network, with the assumption that there is a quarantine policy in place within the network. It will be assumed that the spreading disease is similar to COVID-19 in terms of how the disease is transmitted and how one goes through the diagnosis and recovery of the disease. Furthermore, to what extent a predefined quarantine policy acts as intervention of the spread of the disease is investigated.

2. THEORETICAL FRAMEWORK

Compartmental models are commonly used for predicting the spread of infectious diseases and for comparing various intervention strategies (Xu and Sui (2009)). They help with a deeper understanding of diseases and with policy-making, as real-life experiments are not a feasible option. Additionally, the epidemic modeling metaphor describes a diversity of phenomena, such as cultural dissemination (Axelrod (1997)) and the spread of rumors (Govindankutty and Gopalan (2023)).

In compartmental models each individual within a population is classified into one of the epidemiological compartments. An example is the SIR model, in which one could be in either of the three compartments: Susceptible, Infective, or Recovered (Zanette and Kuperman (2002)). Every individual is susceptible until the first case of infection occurs; the susceptible part of the population could then be infected by the infective part, via contagion. After an originally susceptible individual becomes infective, they go through a designated recovery time before they enter the recovered stage, in which individuals are immune to the infectious disease and would no longer be spreading the disease. Other instances of compartmental models include the SEIR model, where people that are in the latent period are classified to be in the exposed state (Xu and Sui (2009)), and the SIS model, in which infected individuals become susceptible again after the infection time, such that it could be applied to deceases that do not have protective immunity (Wang et al. (2018)).

In recent years, more extensions of compartmental models have been introduced, so that the propagation of diseases could be described more realistically. For example, it is assumed in the SIR model that the infected population will not grow again once it starts to shrink; in other words, the disease dies out after a single wave has occurred (Perakis et al. (2022)). To cope with

the multiple waves of COVID-19, a multiwave SIR model is proposed, in which the disease is segmented into multiple waves by detected time points, and different infection and recovery rates are used for each wave (Perakis et al. (2022)).

Another way to adjust the SIR model is to take the infected but unreported individuals into account. In the SI(Q/F)RD model, infected individuals could enter either the quarantined state or the undetected state, where those in the undetected state have a higher infection rate, a lower death rate, and potentially a higher recovery rate (Deo and Grover (2021)). Furthermore, this model could also be extended with the multiregional assumption. Assuming that a given country is divided into several regions, migrated individuals are taken into consideration when keeping track of the number of susceptible individuals and the number of people who are infected but not diagnosed (Brugnano et al. (2021)).

To try to accommodate quarantine policies and the possibility that an infected individual is not detected of the disease, or that they do not comply with the quarantine policy they are subject to, the SIR model could be extended with additional quarantined states. In this thesis, it is assumed that an individual who is infected and diagnosed of a given disease, as well as the connections of the diagnosed individual within the network (whether susceptible or infective), are requested to go into quarantine. Therefore, two states "Susceptible and Quarantined" and "Infected and Quarantined" are added to the model. When being in either of the quarantined states, one cannot infect or be infected by the rest of the population.

Assuming that the given population is subject to homogeneous mixing, the general structure of the extended SIR model could be defined as follows: let S_t, I_t, and R_t denote at time t the number of individuals that are susceptible, infective, and recovered. $Q_{S,t}$ is defined as the number of individuals that are in the quarantined state and remain susceptible, and $Q_{I,t}$ as the number of quarantined individuals that are previously infected. Then

$$
\begin{aligned}
S_{t+1} - S_t &= -\beta S_t I_t - p_0 p_1 S_t I_t + \gamma Q_{S,t} \\
I_{t+1} - I_t &= \beta S_t I_t - \alpha_1 I_t - p_0 p_1 I_t \\
Q_{S,t+1} - Q_{S,t} &= p_0 p_1 S_t I_t - \gamma Q_{S,t} \\
Q_{I,t+1} - Q_{I,t} &= p_0 p_1 I_t - \alpha_2 Q_{I,t} \\
R_{t+1} - R_t &= \alpha_1 I_t + \alpha_2 Q_{I,t}
\end{aligned}
$$

where β denotes the transmission rate, that is in the case of discrete time, the rate at which an infective individual infects each of their susceptible connections at each unit of time. p_0 denotes the probability that an infected individual is diagnosed of the disease (and thus is required to go into quarantine) and p_1 the probability that they comply with the quarantine policy. α_1 is defined as the rate at which the infective individuals recover each day, and α_2 as for all diagnosed individuals, the rate at which their infected neighbors stop self-quarantining each day. For γ, it denotes the rate of susceptible individuals previously in quarantine stopping self-quarantining each day. The compartmental structure of the model is illustrated in Fig. 1.

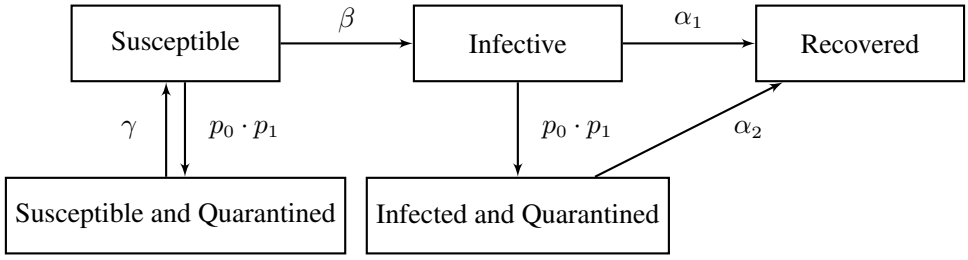

FIGURE 1.—Interactions among the compartments of the extended SIR model.

It is assumed in compartmental models that an infective person could contaminate anyone who is in the susceptible state with equal probability. This homogeneity might be unrealistic for modeling real-life social interactions (Newman (2002)). Network models are formulated such that disease transmission through social interactions could be more realistically shaped; it is done by establishing a network of connections within a population, and small-world networks are in particular a plausible model to mimic social networks in real life (Albert and Barabási (2002)).

In general, small-world networks are network structures in which a few shortcuts are interpolated with a regular lattice; this could be achieved by rewiring a fraction of the edges of the regular lattice randomly (Saramäki and Kaski (2005)). Such networks exhibit high clustering, that is, given a vertex, any of its connections are also likely to be connected. Moreover, they also have small average path lengths, which means that the distance between any pair of vertices is small on average (Zanette and Kuperman (2002)). As real-life networks also exhibit these properties, it is reasonable to model them with small-world networks (Zhang and Zhang (2009)).

The aforementioned models could be used to compare the effectiveness of various vaccination strategies proposed in the literature. For the targeted vaccination strategy, individuals that have the most neighboring vertices within the network receive vaccination (Hartvigsen et al. (2007)). Ring vaccination comprises tracing and immunizing the connecting vertices of an infected individual (Vassallo et al. (2020)). An adapted version of the acquaintance vaccination strategy is to select a fraction of the vertices randomly, and then to vaccinate their immediate neighbors (Xu and Sui (2009)). With this last method, highly connected vertices are more likely to be detected when complete knowledge of the network, as in targeted vaccination, is absent.

In the case of analyzing intervention of the propagation of influenza, which reoccurs on a yearly basis, one strategy could be to vaccinate individuals that were infected in the previous year (Yamin et al. (2014)). It could be argued that the former patients are more likely to be highly connected in the network, and that they are possibly subject to invariable factors, such as genetic or demographic conditions.

If a variation of COVID-19 or an infectious disease that possesses comparable characteristics appears in the future, it is possible to model its transmission and spread within a population with similar processes. By comparing the possible vaccination strategies and examine the effectiveness of a predefined quarantine policy, the results could suggest plausible regulations for the prevention of disease propagation.

3. METHODOLOGY

The social relations within a population could be described by a small-world network model, where the individuals are represented by vertices and the contacts between individuals by edges. Firstly, to generate a small-world network, a regular ring lattice could be created; it contains n nodes located around a circle, each connected to k of its nearest neighbors (Watts and Strogatz (1998)). Secondly, shortcuts between two vertices are generated by rewiring a fraction of edges randomly. While regular lattices display high clustering and long path lengths on average, increasing the rewiring probability leads to a lower average path length (Opsahl et al. (2017)). This could be done by, with probability r, replacing each initial edge (u, v) with a new one, (u, w), where w is an existing node other than u chosen randomly (Hagberg et al. (2008)). This process is iterated until a connected graph is created. Visualization of simulated networks are presented in Fig. 2; the networks contain 20 nodes that have 4 connecting neighbors on average, and they are each rewired with probability $r = 0$, 0.1, and 0.5.

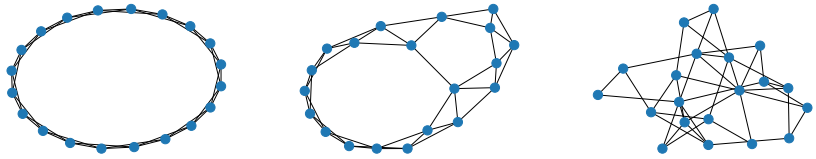

(a) $r = 0$ (b) $r = 0.1$ (c) $r = 0.5$

FIGURE 2.—Simulation of networks where n = 20, k = 4, and r = 0, 0.1, and 0.5

For simulating the spread of the disease using the extended SIR model, here it is assumed in the model that every individual in the network is susceptible before the disease starts to spread. At the beginning of the spread of disease, one randomly selected individual becomes infected. After entering the infective state, one starts to infect their connected vertices that are susceptible with transmission rate β.

With time proceeding in discrete steps, it is assumed here arbitrarily that it takes twelve days for an individual to recover, once they entered the infective state. The median time between the infection and diagnosis of COVID-19 is reported to be 5 days (Yang et al. (2020)). Therefore, here it is assumed that on the sixth day of the 12 days of recovery time, the infected individual could be diagnosed and go into quarantine for 7 days with probability $p_0 \cdot p_1$. If they quarantine themselves as required, each of their neighboring vertices will be quarantined for 12 days, each with probability p_1. During their quarantine period, one cannot infect or be infected by the rest of the population.

When their quarantine period ends, individuals that were once infected progress to the recovered state, and those who were not become susceptible again. Furthermore, if an individual is vaccinated, they enter the recovered state. Eventually, the propagation of the disease ends when there are no longer infected individuals in the population.

To begin with the analysis, the disease spreading on a small-world network without implementation of vaccination is first simulated. For the network model, the number of nodes is set to $n = 1000$, and the average number of connected vertices for each node is $k = 4$. The rewiring probabilities are fixed to 0.1 and 0.5 to simulate two different types of networks.

The propagation of the disease is described by the SIR model with the extension of the quarantined states, where p_1, the probability of an individual quarantining themselves as required, is set to 1. Here the transmission rate β and the detection probability of the disease p_0 are set to 0.319 and 0.26, respectively, which are estimates of the actual probabilities in California, USA using data from Centers for Disease Control and Prevention (CDC) and Johns Hopkins Uni-

versity (Deo and Grover (2021)). Data collected before 19 March 2020, which was the starting date of the first official lockdown in California, were used for the estimation. The parameters used for simulating the networks and the dynamics of the disease are summarized in Table 1.

TABLE I
SETTING OF PARAMETERS FOR SIMULATIONS

Factor	Level(s)
Number of nodes in network n	1000
Average number of neighbors k	4
Rewiring probability r	0.1 and 0.5
Transmission rate β	0.319
Probability of diagnosis p_0	0.26

Scenarios where different vaccination strategies are applied are then simulated, with the first simulation serving as the control. In each of those simulations, either the random vaccination, the targeted vaccination, the adapted acquaintance vaccination, or the ring vaccination strategy is implemented. For each strategy, various percentages of the population are to be vaccinated; the random vaccination, the targeted and adapted acquaintance vaccination are applied before the start of the disease propagation, and the ring vaccination is applied during the process of the spread of the virus, until the designated proportion of the population is immunized. Under the ring vaccination strategy, if an infected individual is diagnosed of the disease, their neighboring vertices are tracked; the neighbors who are remaining susceptible then get vaccinated. After this certain proportion of the population becomes vaccinated, the susceptible neighbors are required to go into quarantine as before.

For evaluating and comparing the effectiveness of the vaccination strategies, several criteria could be used. Firstly, the proportion of the population that has once been infected with the disease under each vaccination strategy is tested, as one could expect effective vaccination to restrict the spread of a disease.

Secondly, the peak number of infected individuals is examined. It reflects the potential amount of medical treatment required at one time (Hartvigsen et al. (2007)). The time to reach peak infection is at last examined. These two properties characterize the (cumulative) curve of the number of infections when different vaccination strategies are applied (Shirley and Rushton (2005)).

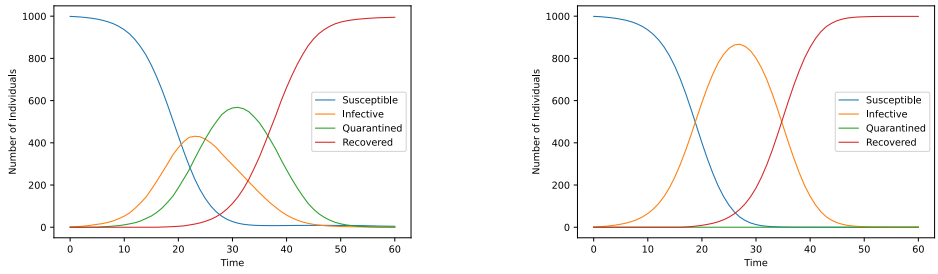

(a) $p_1 = 1$ (b) $p_1 = 0$

FIGURE 3.—SIR epidemic simulation under different values of p_1

Apart from comparing the effectiveness of the vaccination strategies, it is possible to evaluate that of the assumed quarantine policy. By lowering the value of p_1, which was initially set as 1, an epidemic threshold as a function of p_1 could be observed. It could suggest to what extent a government should impose strict quarantine measures on the given population with the aim of restraining the disease from propagating.

The simulation of small-world networks is performed using the Python package NetworkX (Hagberg et al. (2008)), and the algorithm of the extended SIR model is adapted from the algorithms within the Epidemics on Networks (EoN) package (Kiss et al. (2017)). The pseudocode for the extended SIR model is presented in Appendix A.

4. RESULTS

For the results presented in this section, averages of 100 realizations are taken for each combination of the vaccination strategy, the rate at which the given population is vaccinated ρ, the probability that one complies with the quarantine policy p_1, and the rewiring probability r for the simulated networks of 1000 individuals.

The number of individuals in the various states each day within a network with rewiring probability $r = 0.1$ are illustrated in Fig. 3. Two cases are considered: firstly, p_1 is set to 1, meaning that each individual within the population, if requested, goes into quarantine with certainty. Secondly, p_1 is set to 0, which could imply that the quarantine policy is not implemented. Over time, the number of susceptible individuals decreases, and the number of recovered individuals increases. The infective and the quarantined (if $p_1 > 0$) population grows at first and gradually dies out after reaching the maximum size. On average, in the case when $p_1 = 1$, 990 individuals are once infected with the disease, and at most 434 people are in the infective state

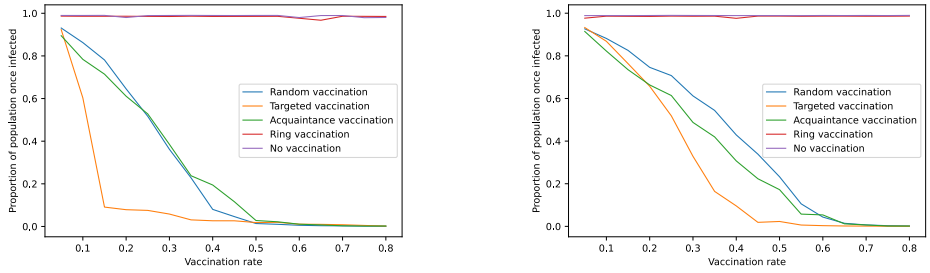

(a) $r = 0.1$ (b) $r = 0.5$

FIGURE 4.—Proportion of population once infected

at the same time. On the other hand, when $p_1 = 0$, the average number of people once infected is 999, and the average peak number of infective individuals is 867.

4.1. *Effectiveness of vaccination strategies*

Firstly, the proportion of the population that has been infected under different vaccination strategies are shown in Fig. 4. Here p_1 is set to 1; simulations are performed for several combinations of the rewiring probability for networks r and the vaccination rate ρ, where $r = 0.1$ or $r = 0.5$, and $\rho = 0.05, 0.10, ..., 0.75, 0.80$. In general, the number of individuals that have been infected with the disease decreases in the vaccination rate. Moreover, the random, the targeted, and the acquaintance vaccination strategies result in lower numbers of total infection in a network with $r = 0.1$, compared to a network containing the same number of people, but with $r = 0.5$.

For a network with rewiring probability $r = 0.1$, the proportion of the population that is once infected is the smallest under targeted vaccination when the vaccination rate is between 0.05 and 0.5 approximately. As for a network with $r = 0.5$, acquaintance vaccination is more effective in terms of lowering the proportion of the population once infected, when the vaccination rate is relatively low (between 0.05 and 0.2 roughly). If higher vaccination rate is allowed for the population, targeted vaccination would be preferred.

In the network with $r = 0.1$, acquaintance vaccination outperforms random vaccination for lower vaccination rates, while random vaccination is more favored for higher vaccination rates. With a higher vaccination rate, targeted vaccination is slightly more effective on the network with higher randomness ($r = 0.5$), rather than on the more regular network ($r = 0.1$).

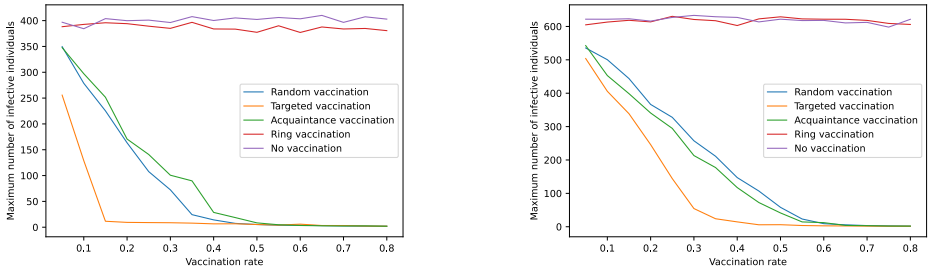

(a) $r = 0.1$ (b) $r = 0.5$

FIGURE 5.—Maximum number of infective individuals

Secondly, under each vaccination strategy, the maximum number of infective individuals during the spread of the disease is shown in Fig.5. Before any vaccination strategy is implemented, the peak size of the infective population is larger for the network with $r = 0.5$ than for that with $r = 0.1$. It is also decreasing in the vaccination rate in the case when random, targeted, or acquaintance vaccination is applied.

In both simulated networks, targeted vaccination is the most effective as to decrease the maximum number of infective individuals. Random vaccination results in a lower level of peak infection than acquaintance does within the network with $r = 0.1$, but the opposite result is obtained for the network with $r = 0.5$.

Thirdly, under random, targeted, and acquaintance vaccination, the number of days it takes for a population to reach the maximum infection level first rises and then declines with the vaccination rate as a general trend. As time until peak infection decreases under each of these vaccination strategies, it falls below that where no vaccination is implemented at some point in time. Random vaccination and acquaintance vaccination lead to more similar trends in both networks. As shown in Fig. 6, before part of the population gets vaccinated, it takes a longer time to reach the peak infection level in the more regular network. Typically, there is a negative and linear relation between the peak infection level and time until peak infection (Xu and Sui (2009)); however, the negative relation is only existent for lower vaccination rates in this case.

Lastly, the duration of the spread of the disease is examined; the results are presented in Fig. 7. Under each vaccination strategy, the duration of infection shows a similar trend as time until peak infection does. Before applying any vaccination strategies, the duration of infection is longer in the more regular network.

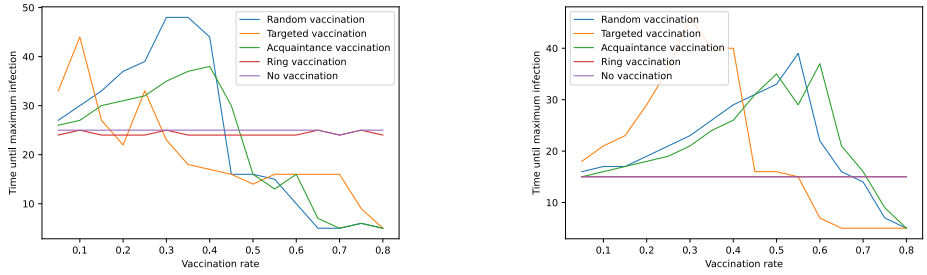

(a) $r = 0.1$ (b) $r = 0.5$

FIGURE 6.—Time until maximum infection

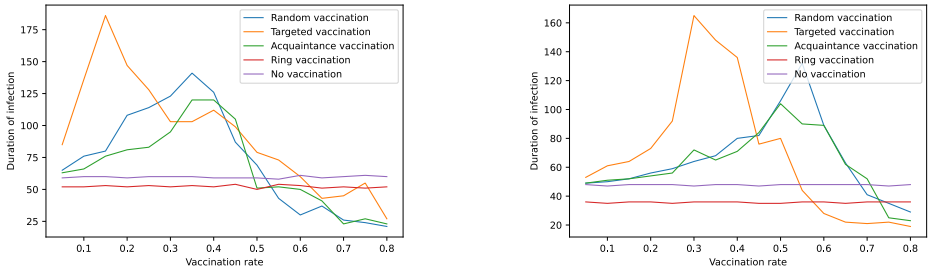

(a) $r = 0.1$ (b) $r = 0.5$

FIGURE 7.—Duration of infection

The ring vaccination strategy is not effective as to lowering the proportion of the population once infected or the maximum number of infective individuals (Figs. 4 and 5). As shown in Fig.8, when ring vaccination is applied, the actual number of vaccinated individuals is a lot smaller than the designated number of individuals to be vaccinated. The simulations terminate before the goal vaccination rate is reached. Nonetheless, ring vaccination results in a shorter duration of the disease propagation in both networks (Fig. 7).

4.2. *Effects of predefined quarantine policy and individual willingness to self-quarantine*

In Fig. 9, the effects of lowering the probability that each individual complies with the quarantine policy p_1 on the effectiveness of vaccination strategies are illustrated. The targeted vaccination and the network with $r = 0.1$ is chosen for demonstration.

The proportion of population once infected increases as p_1 decreases, and the effect is more dramatic for vaccination rates $\rho = 0.1$ and $\rho = 0.2$. The same effect could be observed for the

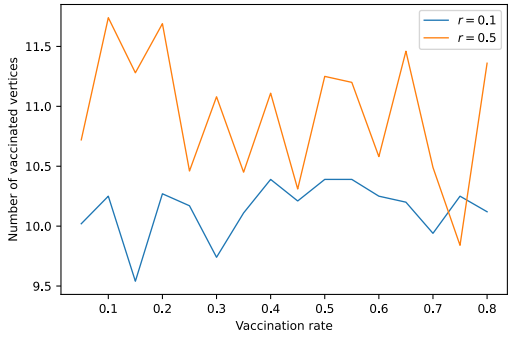

FIGURE 8.—Number of vaccinated vertices under ring vaccination

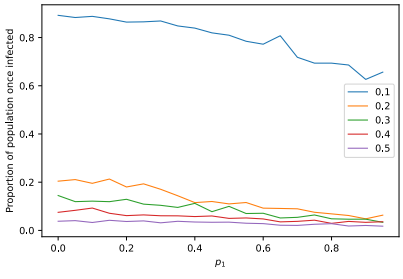

(a) Proportion of population once infected

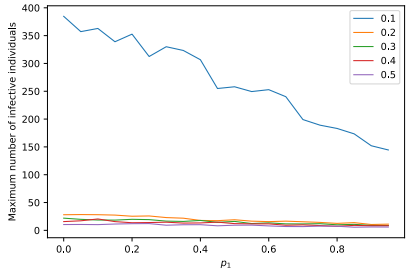

(b) Maximum number of infective individuals

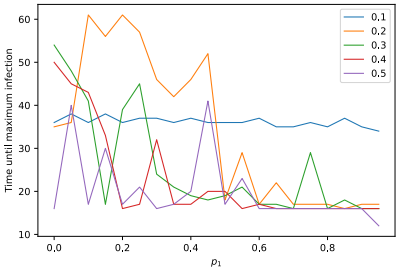

(c) Time until maximum infection

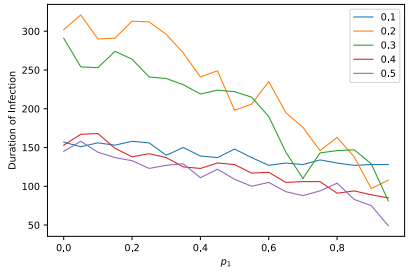

(d) Duration of infection

FIGURE 9.—Simulation results under targeted vaccination within network with rewiring probability $r = 0.1$, for vaccination rates $\rho = 0.1, 0.2, ..., 0.5$

maximum number of infective individuals; for $\rho = 0.1$, the peak level of infection increases the most. For $\rho = 0.2, 0.3, 0.4$, and 0.5, the fluctuations in time until maximum infection become larger as p_1 decreases; however, the effect of changes in the value of p_1 when $\rho = 0.1$ is not

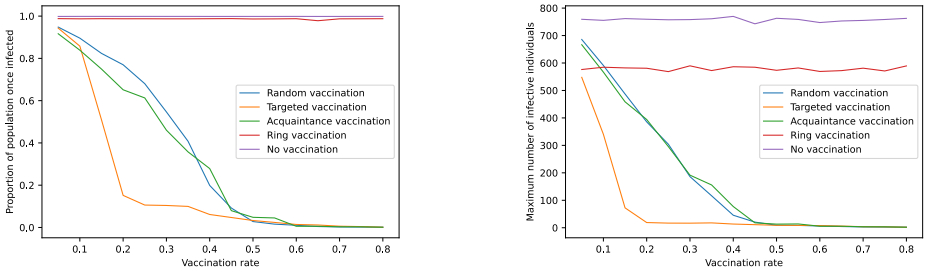

(a) Proportion of population once infected

(b) Maximum number of infective individuals

FIGURE 10.—Simulation results within network with rewiring probability $r = 0.1$, for $p_1 = 0.3$

obvious. Regarding the duration of infection, it increases with lowering values of p_1, and the increase is larger when $\rho = 0.2$ and when $\rho = 0.3$.

Results for evaluating and comparing the aforementioned vaccination strategies are simulated in the case when p_1 is set to 0.3, representing a scenario when individuals in the network are less likely to self-quarantine if requested. As illustrated in Fig. 10, in the network with $r = 0.1$, there is no obvious effect of the lower p_1 on the size of the once infected population. However, the peak size of the infective population increases substantially under ring vaccination and almost doubled when no vaccination is given within the population. As when $p_1 = 1$, it does not decrease in the vaccination rate, unlike under other vaccination strategies.

Furthermore, all vaccination strategies result in similar time until peak infection level and a similar duration of infection as in the case when $p_1 = 1$, for the various values of vaccination rates. The visualization is shown in Appendix B, Fig. B.1. The results for the network with $r = 0.5$ is presented in Appendix B, Fig. B.2.

5. DISCUSSION

In previous studies, the proportion of the once infected population relative to the initially non-vaccinated population is used (Xu and Sui (2009); Zanette and Kuperman (2002)), rather than that relative to the whole population. However, the former is not entirely applicable in this setting. Under ring vaccination, individuals receive vaccination during the process of the spread of the disease; therefore, the non-vaccinated population consists of all 1000 individuals for every vaccination rate in this case. On the other hand, under random, targeted, and acquaintance vaccination, a fraction of the population receives vaccination before the simulations start; the

size of the non-vaccinated population then becomes smaller and the results are not comparable among all vaccination strategies.

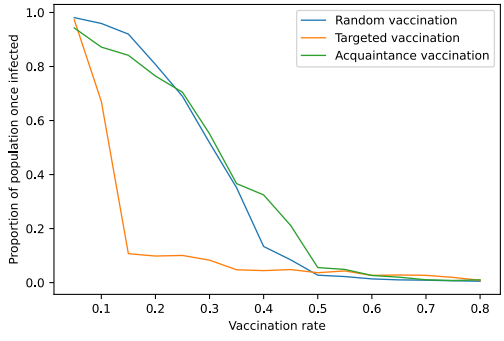

FIGURE 11.—Proportion of non-vaccinated population once infected in a network with $r = 0.1$ and $p_1 = 1$

Fig. 11 illustrates the proportion of the non-vaccinated population that has once been infected when random, targeted, or acquaintance vaccination is implemented in the network with $r = 0.1$. The trends with the increasing vaccination rate are similar to those in Fig. 4.

The small-world properties, which are high clustering and small average path lengths, are observed in networks with a rewiring probability ranging from $r = 0.001$ to $r = 0.1$ (Menezes et al. (2017)). Here rewiring probabilities $r = 0.1$ and $r = 0.5$ are set for the networks, because the duration of the spread of the disease failed to be calculated for lower rewiring probabilities when the algorithm for the extended SIR model is used.

There could be several potential reasons why the predetermined quarantine policy is ineffective in terms of lowering the proportion of the once infected population (Figs. 4a and 10a). For example, firstly, the probability of detection of the disease p_0 is fixed to 0.26, which is relatively low. Secondly, rewired networks where a vertex has four connected vertices on average are used; more individuals could be requested to go into quarantine if the average number of connected vertices for each individual is increased.

Similar to the quarantine policy, the effectiveness of ring vaccination could suffer from the low probability of diagnosis and a relatively small number of connections within the assumed networks. Additionally, for a diagnosed individual, their neighbors are likely to already be infective or quarantined; the chances of finding a neighboring and susceptible individual is therefore lower when a quarantine policy is in place. This could cause the population to not be

vaccinated up to the desired vaccinated rate. Further investigation could be done on networks in which the nodes have a higher average number of connections k.

6. CONCLUSION

A network model and an extended SIR model with a quarantined compartment are used to simulate the dynamics of the spread of a disease. The disease is assumed to bear similar characteristics as those of COVID-19, which are the transmission rate, the probability of diagnosis, and the median time span between infection and diagnosis in particular. For each of the simulations, the interaction between the rewiring probability for the networks, the type of vaccination strategy, the aimed vaccination rate, and the rate of compliance with the quarantine policy affect the dynamics of the disease propagation.

Based on the settings of the models and the simulation results, it could be concluded that targeted vaccination is the most effective for reducing the size of the population that has been infected before, except for the case of a low vaccination rate combined with a low rewiring probability for the network. In that case, acquaintance vaccination is shown to be more effective. Targeted vaccination is also shown to be the most effective in terms of lowering the peak infection level of the disease. In general, random vaccination and acquaintance vaccination give similar results given each level of vaccination rate. As for ring vaccination, it is not effective as intervention of the disease propagation, especially when the probability of compliance with the quarantine policy is high.

As the probability of each individual complying with the quarantine policy decreases, both the proportion of the population once infected and the peak infection level increases; for both criteria, the increment is more prominent in the case with a lower vaccination rate. The fluctuations in time until peak infection is larger for small probabilities of compliance with the quarantine policy. Lastly, the duration of the spread of the disease increases as the probability of compliance with the quarantine policy lowers.

In the setting of the extended SIR model, the transmission rate β is constant for all connections between two vertices. However, the transmission rate can differ in real life for each pair of vertices, according to for example the strength of individuals' immune system. This could possibly be taken into consideration in further research. The model could also be accounting for the fact that in the case of COVID-19, one could still be infected with the disease after recovering. Therefore, individuals who have recovered could return to the susceptible state of the model, and this could capture the dynamics of the disease more realistically.

APPENDIX A: PSEUDOCODE FOR EXTENDED DISCRETE SIR MODEL

inputs:

Graph generated using NetworkX G
Transmission rate β
Probability that an infective individual is diagnosed p_0
Probability that an individual self-quarantines if requested p_1
Set of initially infective individuals in the network *initial infecteds*
Set of initially recovered/vaccinated individuals *initial recovereds*
Starting time unit of simulation *tmin*
Ending time unit of simulation *tmax*

function SIMPLE TEST TRANSMISSION(u, v, β)
    return random number between 0.0 and 1.0 $< \beta$
end function

function SIMPLE TEST DETECTION(u, p_0)
    return random number between 0.0 and 1.0 $< p_0$
end function

function SIMPLE TEST QUARANTINE(u, p_0, p_1)
    return random number between 0.0 and 1.0 $< p_0 \cdot p_1$
end function

function SIMPLE TEST QUARANTINE NEIGHBORS(u, p_1)
    return random number between 0.0 and 1.0 $< p_1$
end function

function DISCRETE SIR(G, β, p_0, p_1, *initial infecteds*, *initial recovereds*, *tmin*, *tmax*)
    $N, t \leftarrow$ number of nodes in network, list with value *tmin*
    if *initial recovereds* is not empty set **then**
        $S \leftarrow$ list with value ($N-$ length of *initial infecteds* $-$ length of *initial recovereds*)
    else
        $S \leftarrow$ list with value ($N-$ length of *initial infecteds*)
    end if
    $I \leftarrow$ list with value (length of *initial infecteds*)
    $Q \leftarrow$ list with value 0
    if *initial recovereds* is not empty set **then**
        $R \leftarrow$ list with value (length of *initial recovereds*)
    else

25: $S \leftarrow$ list with value 0
26: **end if**

27: *susceptibles* $\leftarrow$ empty set
28: **for** $u \in \{1, \ldots, N\}$ **do**
29: **if** *initial recovereds* is not empty set **then**
30: **if** u is not in *initial infecteds* or *initial recovereds* **then**
31: add u to *susceptibles*
32: **end if**
33: **else**
34: **if** u is not in *initial infecteds* **then**
35: add u to *susceptibles*
36: **end if**
37: **end if**
38: **end for**
39: *infection time* $\leftarrow$ set of length N with values `NaN`
40: *infectives* $\leftarrow$ set of *initial infecteds*
41: *quarantineds* $\leftarrow$ empty set
42: qs_s, $qs_i \leftarrow$ empty set, empty set
43: *quarantine time* $\leftarrow$ set of length N with values `NaN`
44: **if** *initial recovereds* is not empty set **then**
45: *recovereds* $\leftarrow$ set of *initial recovereds*
46: **else**
47: *recovereds* $\leftarrow$ empty set
48: **end if**
49: `count` $\leftarrow 0$

50: **while** *infectives* is not empty set and last element of $t <$ *tmax* **do**
51: *new susceptibles*, *new infectives* $\leftarrow$ empty set, empty set
52: *new quarantineds*, *new* qs_s, *new* $qs_i \leftarrow$ empty set, empty set, empty set
53: *new recovereds* $\leftarrow$ empty set

$\triangleright\ S \to I$

54: **for all** u in *infectives* **do**
55: **for all** v in set of neighbors of u **do**
56: **if** v is in *susceptibles* and not in *new infectives* **then**
57: **if** SIMPLE TEST TRANSMISSION(u, v, β) **then**
58: add v to *new infectives*
59: v^{th} element of *infection time* $\leftarrow$ last element of t

60: count ← count+1
61: **end if**
62: **end if**
63: **end for**
64: **end for**
65: *susceptibles* ← *susceptibles*−*new infectives*
66: *infectives* ← *infectives* union *new infectives*

▷ $I \to Q$ (quarantined) or $S \to Q$

67: **for all** u in *infectives* **do**
68: **if** (last element of t) − (u^{th} element of *infection time*) $= 5$ and u is not in *quarantineds*, *quarantineds*, qs_i, or *new* qs_i and SIMPLE TEST QUARANTINE(u, p_0, p_1) **then**
69: add u to *new quarantineds*
70: u^{th} element of *quarantine time* ← last element of t
71: **for all** v in set of neighbors of u **do**
72: **if** v is not in *quarantineds*, *new quarantineds*, qs_s, *new* qs_s, qs_i, or *new* qs_i and SIMPLE TEST QUARANTINE NEIGHBORS(v, p_1) **then**
73: **if** v is in *susceptibles* **then**
74: add v to *new* qs_s
75: v^{th} element of *quarantine time* ← last element of t
76: **else if** v is in *infectives* **then**
77: add v to *new* qs_i
78: v^{th} element of *quarantine time* ← last element of t
79: **end if**
80: **end if**
81: **end for**
82: **end if**
83: **end for**
84: *infectives* ← *infectives*−*new quarantineds*−*new* qs_i
85: *susceptibles* ← *susceptibles*−*new* qs_s
86: *quarantineds* ← *quarantineds* union *new quarantineds*
87: qs_s ← qs_s union *new* qs_s
88: qs_i ← qs_i union *new* qs_i

▷ $I \to R$, $Q \to R$, or $Q \to S$

89: *new susceptibles* (q_s) ← empty set
90: *new recovereds* (q) ← empty set
91: *new recovereds* (q_i) ← empty set

92: **for all** u in *infectives* **do**
93: **if** (last element of t) $-$ (u^{th} element of *infection time*) $= 12$ **then**
94: add u to *new recovereds*
95: **end if**
96: **end for**
97: **for all** u in *quarantineds* **do**
98: **if** (last element of t) $-$ (u^{th} element of *quarantine time*) $= 7$ **then**
99: add u to *new recovereds (q)*
100: **end if**
101: **end for**
102: **for all** u in qs_s **do**
103: **if** (last element of t) $-$ (u^{th} element of *quarantine time*) $= 12$ **then**
104: add u to *new susceptibles* (q_s)
105: **end if**
106: **end for**
107: **for all** u in qs_i **do**
108: **if** (last element of t) $-$ (u^{th} element of *quarantine time*) $= 12$ **then**
109: add u to *new recovereds* (q_i)
110: **end if**
111: **end for**
112: *susceptibles* $\leftarrow$ *susceptibles* union *new susceptibles* (q_s)
113: *infectives* $\leftarrow$ *infectives* $-$ *new recovereds*
114: *quarantineds* $\leftarrow$ *quarantineds* $-$ *new recovereds (q)*
115: $qs_s \leftarrow qs_s -$ *new susceptibles* (q_s)
116: $qs_i \leftarrow qs_i -$ *new recovereds* (q_i)
117: *recovereds* $\leftarrow$ *recovereds* union *new recovereds* union *new recovereds (q)* union *new recovereds* (q_i)

118: append length of *susceptibles* to S
119: append length of *infectives* to I
120: append (length of *quarantineds*) + (length of qs_s) + (length of qs_i) to Q
121: append length of *recovereds* to S
122: append (last element of t) $+ 1$ to t
123: **end while**
124: **return** $t, S, I, Q, R,$ `count`
125: **end function**

APPENDIX B: FIGURES

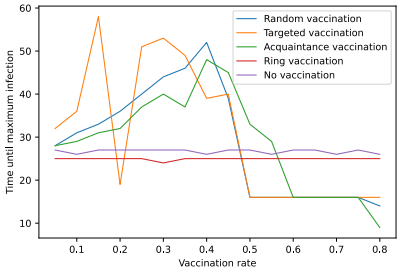

(a) Time until maximum infection

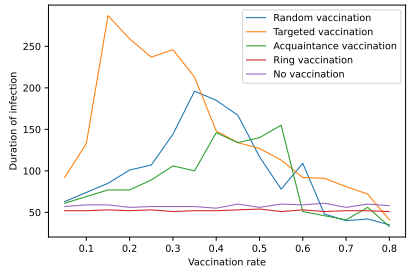

(b) Duration of infection

FIGURE B.1.—Simulation results within network with rewiring probability $r = 0.1$, for $p_1 = 0.3$

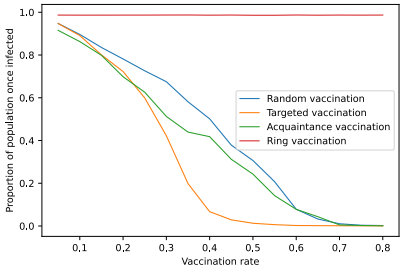

(a) Proportion of population once infected

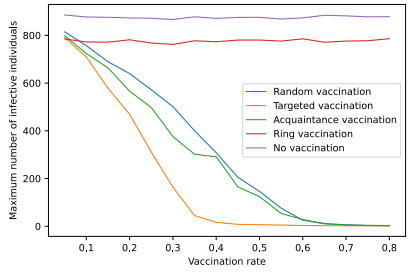

(b) Maximum number of infective individuals

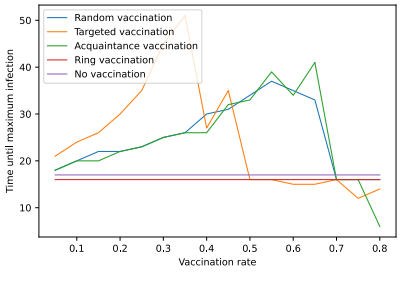

(c) Time until maximum infection

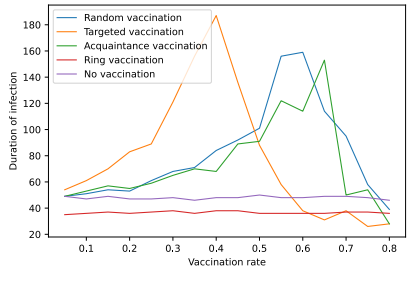

(d) Duration of infection

FIGURE B.2.—Simulation results within network with rewiring probability $r = 0.5$, for $p_1 = 0.3$

REFERENCES

ALBERT, RÉKA AND ALBERT-LÁSZLÓ BARABÁSI (2002): "Statistical mechanics of complex networks," *Reviews of modern physics*, 74 (1), 47. [6]

AXELROD, ROBERT (1997): "The dissemination of culture: A model with local convergence and global polarization," *Journal of conflict resolution*, 41 (2), 203–226. [4]

BRUGNANO, LUIGI, FELICE IAVERNARO, AND PAOLO ZANZOTTERA (2021): "A multiregional extension of the SIR model, with application to the COVID-19 spread in Italy," *Mathematical methods in the applied sciences*, 44 (6), 4414–4427. [3, 4, 5]

DEO, VISHAL AND GURPRIT GROVER (2021): "A new extension of state-space SIR model to account for underreporting–an application to the COVID-19 transmission in California and Florida," *Results in Physics*, 24, 104182. [5, 9]

GOVINDANKUTTY, SREERAAG AND SHYNU PADINJAPPURATHU GOPALAN (2023): "SEDIS—A Rumor Propagation Model for Social Networks by Incorporating the Human Nature of Selection," *Systems*, 11 (1), 12. [4]

HAGBERG, ARIC, PIETER SWART, AND DANIEL SCHULT (2008): "Exploring network structure, dynamics, and function using NetworkX," Tech. rep., Los Alamos National Lab.(LANL), Los Alamos, NM (United States). [7, 10]

HARTVIGSEN, G., J.M. DRESCH, A.L. ZIELINSKI, A.J. MACULA, AND C.C. LEARY (2007): "Network structure, and vaccination strategy and effort interact to affect the dynamics of influenza epidemics," *Journal of theoretical biology*, 246 (2), 205–213. [7, 9]

KISS, ISTVAN Z., JOEL C. MILLER, AND PÉTER L. SIMON (2017): *Mathematics of Epidemics on Networks: from Exact to Approximate Models*, IAM, Springer. [10]

MAY, ROBERT M. AND ROY M. ANDERSON (1984): "Spatial heterogeneity and the design of immunization programs," *Mathematical Biosciences*, 72 (1), 83–111. [3]

MENEZES, MOZART B.C., SEOKJIN KIM, AND RONGBING HUANG (2017): "Constructing a Watts-Strogatz network from a small-world network with symmetric degree distribution," *PloS one*, 12 (6), e0179120. [16]

NEWMAN, MARK E.J. (2002): "Spread of epidemic disease on networks," *Physical review E*, 66 (1), 016128. [6]

OPSAHL, TORE, ANTOINE VERNET, TUFOOL ALNUAIMI, AND GERARD GEORGE (2017): "Revisiting the small-world phenomenon: Efficiency variation and classification of small-world networks," *Organizational Research Methods*, 20 (1), 149–173. [7]

PERAKIS, GEORGIA, DIVYA SINGHVI, OMAR SKALI LAMI, AND LEANN THAYAPARAN (2022): "COVID-19: A multiwave SIR-based model for learning waves," *Production and Operations Management*. [4, 5]

SARAMÄKI, JARI AND KIMMO KASKI (2005): "Modelling development of epidemics with dynamic small-world networks," *Journal of Theoretical Biology*, 234 (3), 413–421. [6]

SHIRLEY, MARK D.F. AND STEVE P. RUSHTON (2005): "The impacts of network topology on disease spread," *Ecological Complexity*, 2 (3), 287–299. [9]

VASSALLO, LAUTARO, MATÍAS A DI MURO, DEBMALYA SARKAR, LUCAS D VALDEZ, AND LIDIA A BRAUNSTEIN (2020): "Ring vaccination strategy in networks: A mixed percolation approach," *Physical Review E*, 101 (5), 052309. [7]

WANG, WEIMING, YONGLI CAI, ZUQIN DING, AND ZHANJI GUI (2018): "A stochastic differential equation SIS epidemic model incorporating Ornstein–Uhlenbeck process," *Physica A: Statistical Mechanics and its Applications*, 509, 921–936. [4]

WATTS, DUNCAN J. AND STEVEN H. STROGATZ (1998): "Collective dynamics of 'small-world' networks," *Nature (London)*, 393 (6684), 440–442. [7]

XU, ZENGWANG AND DANIEL Z. SUI (2009): "Effect of small-world networks on epidemic propagation and intervention," *Geographical Analysis*, 41 (3), 263–282. [4, 7, 12, 15]

YAMIN, DAN, ARIEH GAVIOUS, EYAL SOLNIK, NADAV DAVIDOVITCH, RAN D. BALICER, ALISON P. GALVANI, AND JOSEPH S. PLISKIN (2014): "An innovative influenza vaccination policy: targeting last season's patients," *PLoS Computational Biology*, 10 (5), e1003643. [7]

YANG, XIAOBO, YUAN YU, JIQIAN XU, HUAQING SHU, HONG LIU, YONGRAN WU, LU ZHANG, ZHUI YU, MINGHAO FANG, TING YU, ET AL. (2020): "Clinical course and outcomes of critically ill patients with SARS-CoV-2 pneumonia in Wuhan, China: a single-centered, retrospective, observational study," *The lancet respiratory medicine*, 8 (5), 475–481. [8]

YANG, YONG AND PETER M. ATKINSON (2008): "Individual space–time activity-based model: a model for the simulation of airborne infectious-disease transmission by activity-bundle simulation," *Environment and Planning B: Planning and Design*, 35 (1), 80–99. [3]

ZANETTE, DAMIÁN H. AND MARCELO KUPERMAN (2002): "Effects of immunization in small-world epidemics," *Physica A: Statistical Mechanics and its Applications*, 309 (3-4), 445–452. [4, 6, 15]

ZHANG, ZHIHUA AND JIANZHI ZHANG (2009): "A big world inside small-world networks," *PloS one*, 4 (5), e5686. [6]